

Yapay ve Gerçek Sinir Ağları

Matematik Kullanabilmenin Faydaları

Neslihan Serap ŞENGÖR

İTÜ Maslak, Ekim, 2019

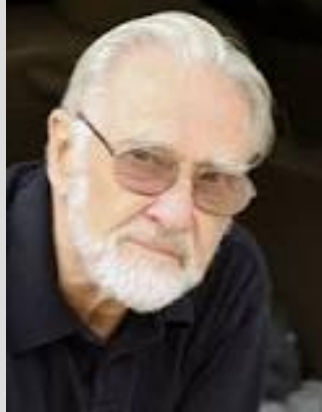


İstanbul Teknik Üniversitesi
Sinirbilim Modelleme ve Araştırma Grubu



İstanbul Teknik Üniversitesi
Elektronik ve haberleşme Mühendisliği Bölümü

Bir psikolog fizikçileri niçin kıskanır.....



1964

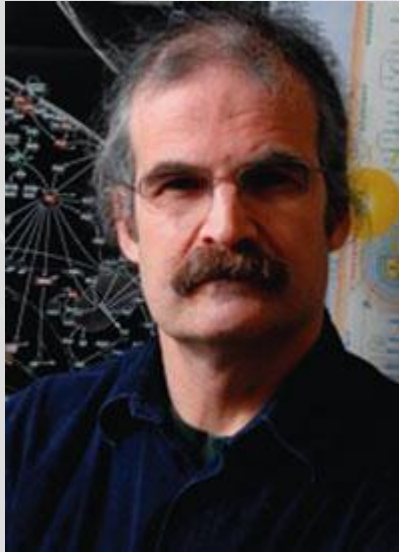
THE MATHEMATICS USED IN MATHEMATICAL PSYCHOLOGY

R. DUNCAN LUCE, University of Pennsylvania

Introduction. The main issue in applying mathematics to psychological problems today, and most likely for some time to come, is the formulation of these problems in mathematical terms. The solution of difficult but well-formulated mathematical problems and the analysis of complex applied problems in terms of precise and well-confirmed theories are more secondary efforts. We do not yet have the basic concepts and variables staked out in a way that makes the introduction of mathematics the relatively straightforward business that it has become in much of physical science. We are in a situation somewhat analogous to sixteenth, or hopefully seventeenth, century physics, but the analogy is far from complete. We resemble the early physicists in our effort, often fumbling and always slow, to isolate and purify the fundamental variables from the myriad, vague, commonsense psychological ideas and concepts. We differ in the range of techniques available to us. The modern electronics technology, including high speed computers, provides us with a control over experimental conditions and a computational capacity for data analysis incomparably more extensive and subtle than those with which the early physicists had to contend. In addition, most of the mathematics and statistics we now use was quite unknown three centuries ago.

R.Duncan Luce
1925-2012

Biyologlar da kıskanmakta....



Yuri Lazebnik

*Biochemistry (Moscow), Vol. 69, No. 12, 2004, pp. 1403-1406.
Copyright © 2002 by CELL PRESS.*

DISCUSSIONS

Can a Biologist Fix a Radio? — or, What I Learned while Studying Apoptosis

Y. Lazebnik

*Cold Spring Harbor Laboratory, Cold Spring Harbor,
New York 11724, USA; E-mail: lazebnik@cshl.org*

This article by Yu. Lazebnik, “Can a Biologist Fix a Radio? — or, What I Learned while Studying Apoptosis” has already been published in English (*Cancer Cell*, 2002, 2, 179-182) and in Russian (*Uspekhi Gerontologii*, 2003, No. 12, 166-171). Nevertheless, we have undertaken its secondary publication in our journal for two reasons: first, our journal has different readers, and, second, the great significance of this manifest of Yuri Lazebnik. The author in bright and clever form shows the emerging necessity to create formalized language designed to describe complicated systems of regulation of biochemical processes in living cells. The article is published with permission of *Cancer Cell* and *Uspekhi Gerontologii*.

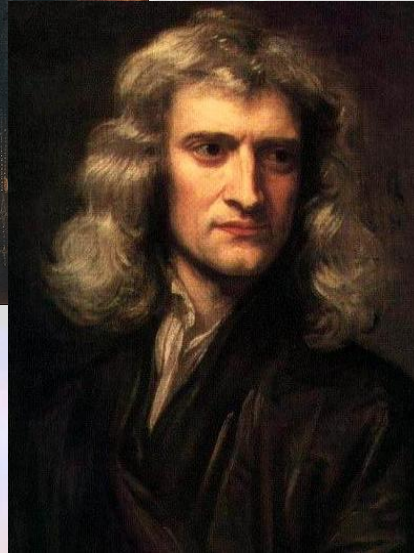
Editor-in-Chief of Biokhimiya/Biochemistry (Moscow) V. P. Skulachev

Matematik: Doğanın kitabının dili



Galileo Galilei
1564-1642

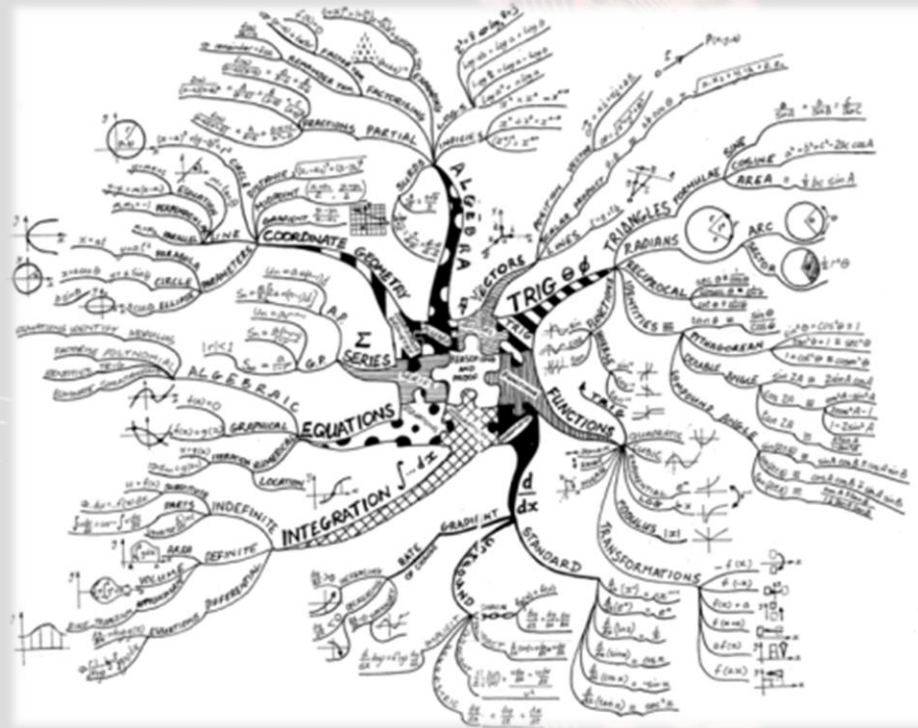
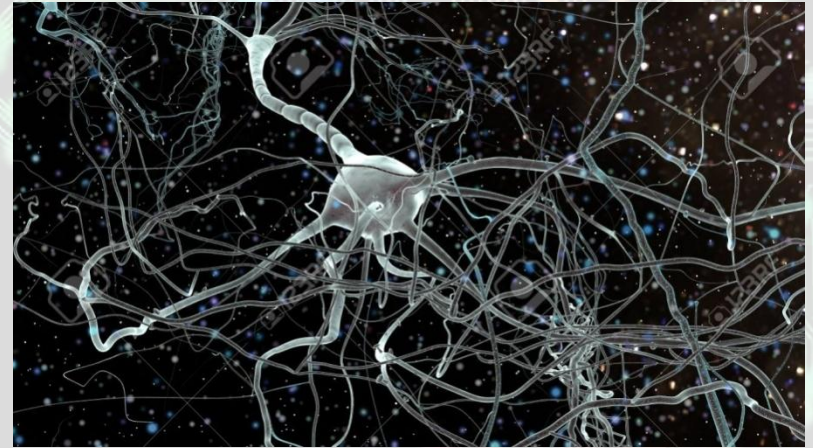
$$x = \frac{1}{2}gt^2$$



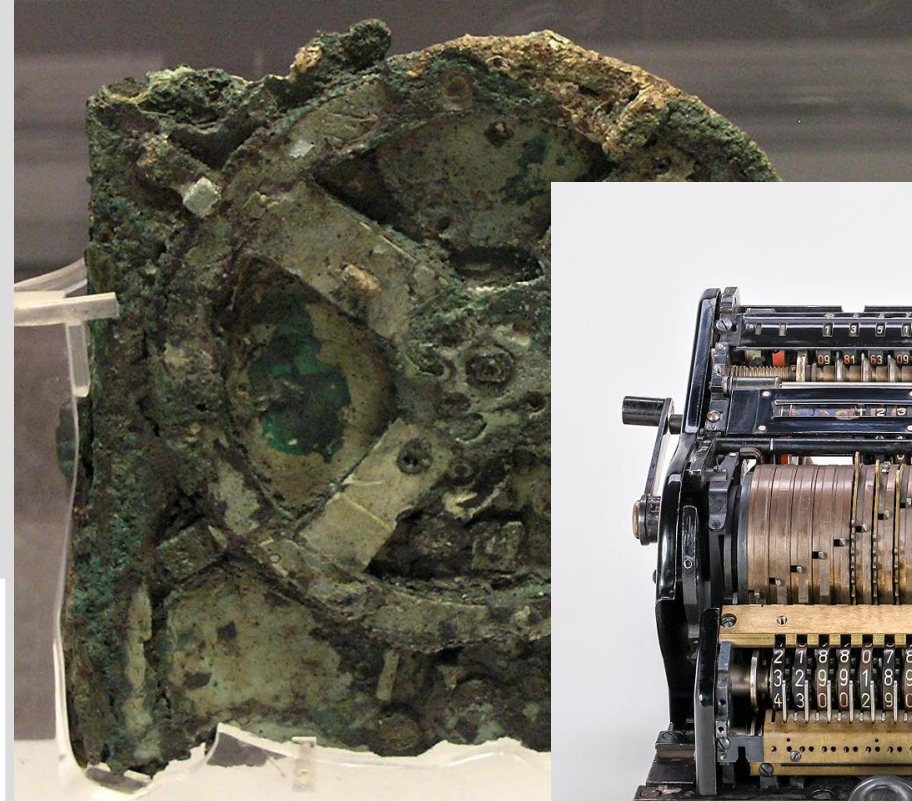
Isaac Newton
1643-1727

$$F = ma$$

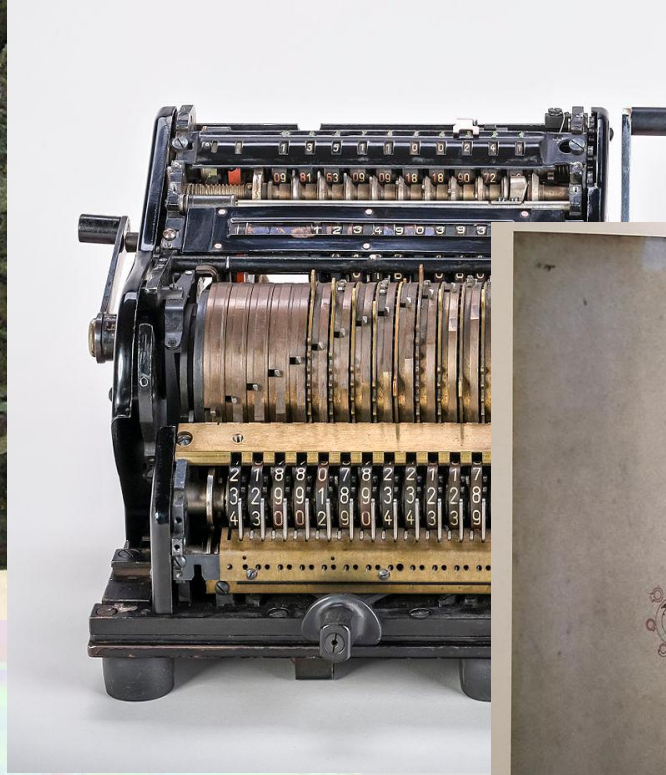
$$F = m \frac{d^2x}{dt^2}$$



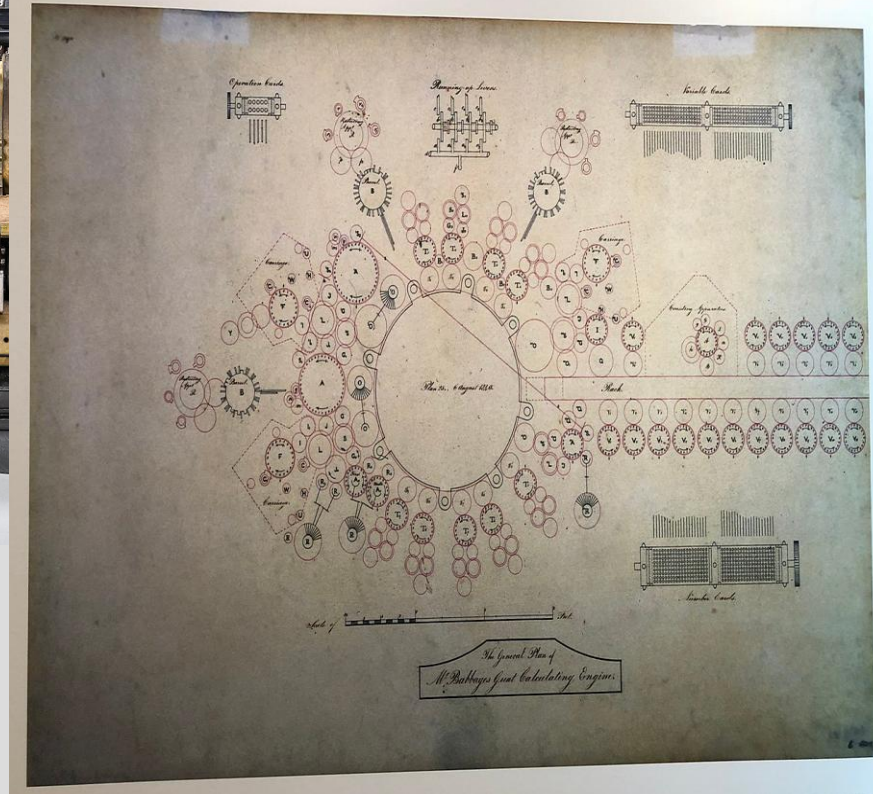
Antikythera Düzeneği MÖ 150-100



Leibniz Çarkı 1673



Analitik Makine 1833



MIND

A QUARTERLY REVIEW

OF

PSYCHOLOGY AND PHILOSOPHY

I.—COMPUTING MACHINERY AND
INTELLIGENCE

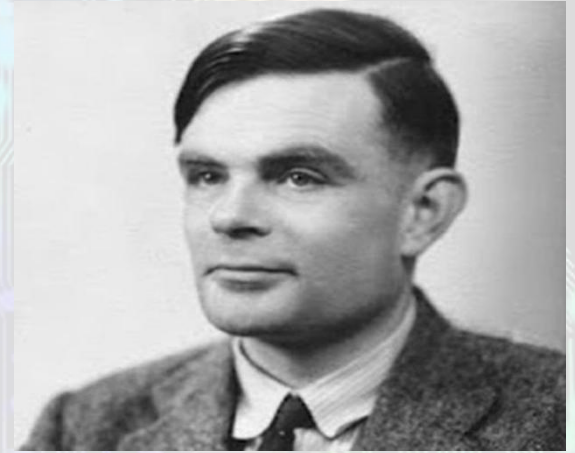
BY A. M. TURING

1. *The Imitation Game.*

I PROPOSE to consider the question, 'Can machines think?' This should begin with definitions of the meaning of the terms 'machine' and 'think'. The definitions might be framed so as to reflect so far as possible the normal use of the words, but this attitude is dangerous. If the meaning of the words 'machine' and 'think' are to be found by examining how they are commonly used it is difficult to escape the conclusion that the meaning and the answer to the question, 'Can machines think?' is to be sought in a statistical survey such as a Gallup poll. But this is absurd. Instead of attempting such a definition I shall replace the question by another, which is closely related to it and is expressed in relatively unambiguous words.

The new form of the problem can be described in terms of a game which we call the 'imitation game'. It is played with three people, a man (A), a woman (B), and an interrogator (C) who may be of either sex. The interrogator stays in a room apart from the other two. The object of the game for the interrogator is to determine which of the other two is the man and which is the woman. He knows them by labels X and Y, and at the end of the game he says either 'X is A and Y is B' or 'X is B and Y is A'. The interrogator is allowed to put questions to A and B thus:

C: Will X please tell me the length of his or her hair?
Now suppose X is actually A, then A must answer. It is A's



Alan Turing
1912-1954

İnsan tarzı zekayı mekanikleştirme
olasılığı

Makineler düşünebilir mi? Sorusu
yerine Turing testi

'Zeki' bilgisayara ulaşma olasılığı aleyine
savlar

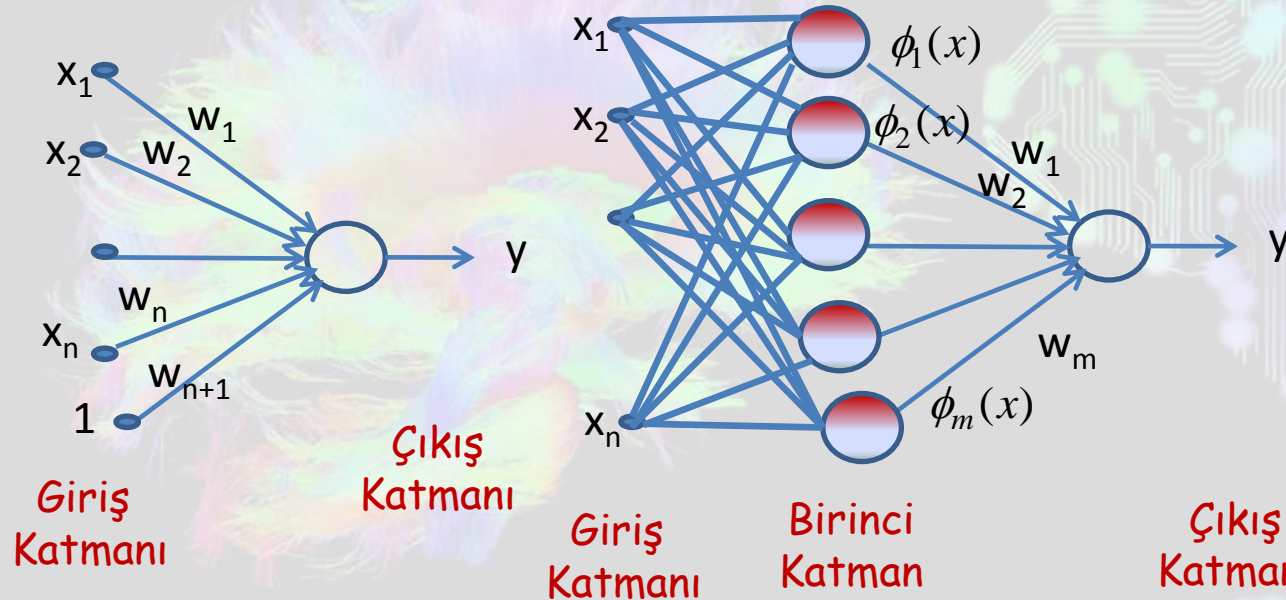
Yetişkin zihnini taklit etme yerine çocuk
zihnini taklit eden programı eğitme

Yapay Zeka Dartmouth Yaz okulu 1956



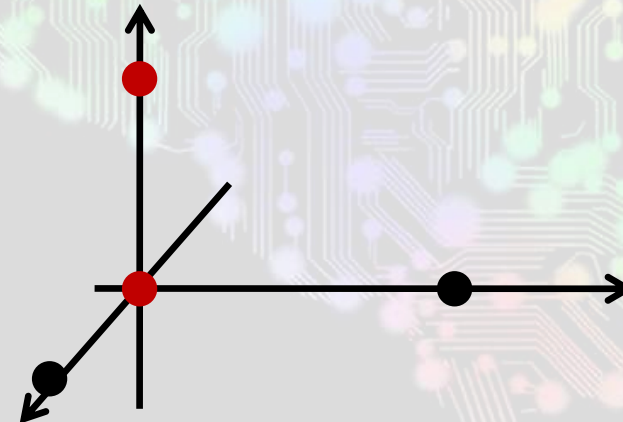
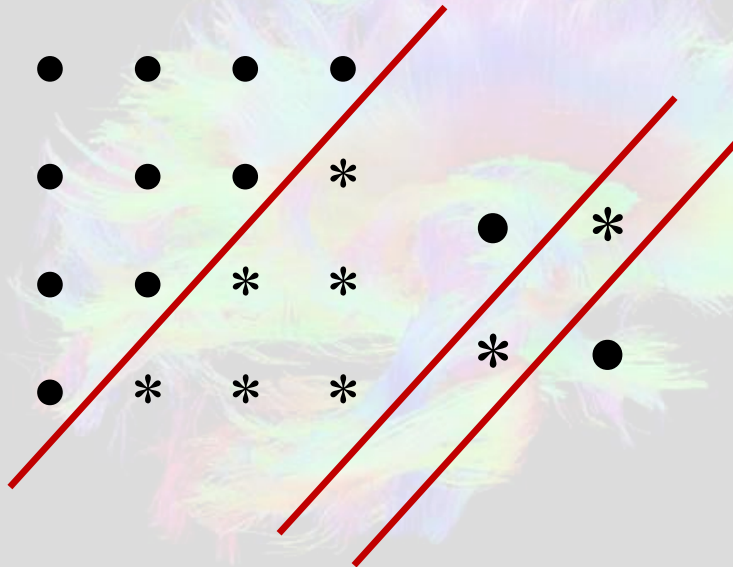
Walter Pitts: Sayın Farley, Clark, Selfridge ve Dinneen sinir sistemini taklit ederlerken, Sayın Newell, geleneksel olarak zihin denilen, nihai sebepler, sebepler hiyerarşisini taklit etmeyi tercih ediyor. Sonunda hepsi hiç şüphesiz aynı kapiya çıkacak. *

Perceptron 1958



Frank Rosenblatt
1928-1971

Sabit ağırlıklar, sabit fonksiyonlar
Bağlantı ağırlıkları, eğitim kümesi ile belirlenen tek bir nöron



ADALINE-MADALINE 1960

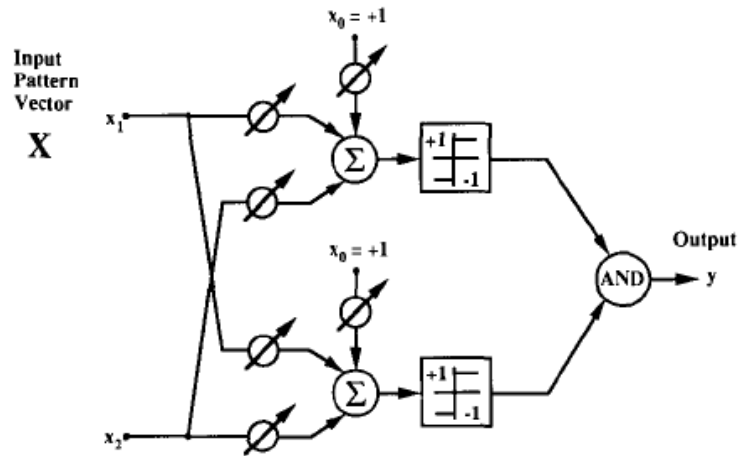


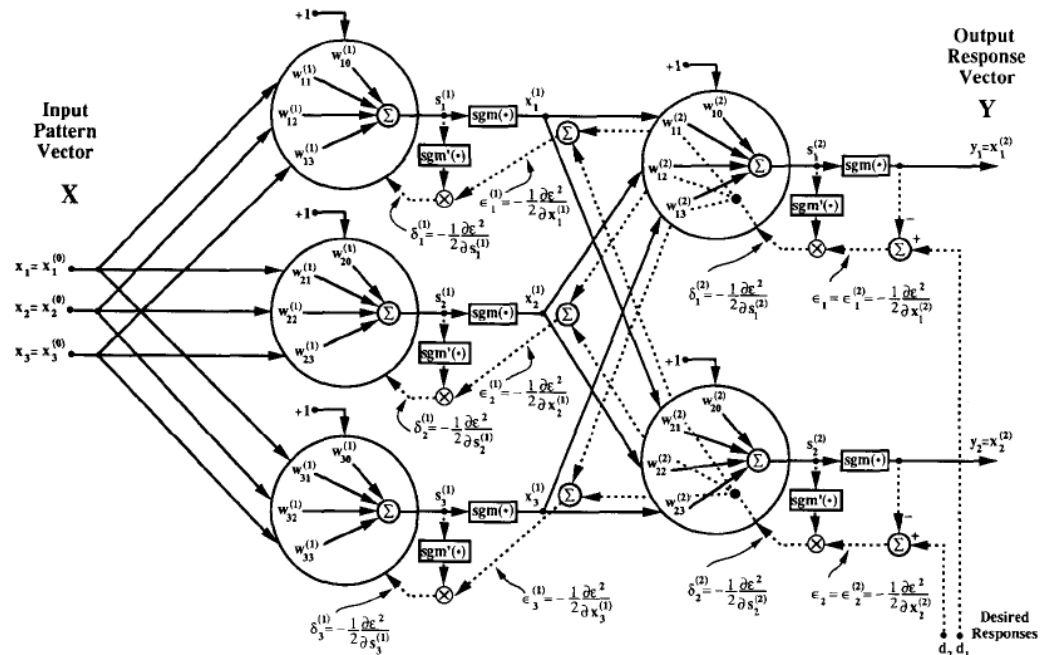
Fig. 8. Two-Adaline form of Madaline.



M.T. Hoff
1937-



Bernard Widrow
1929-



Example two-layer backpropagation network architecture.

Neocognitron 1983

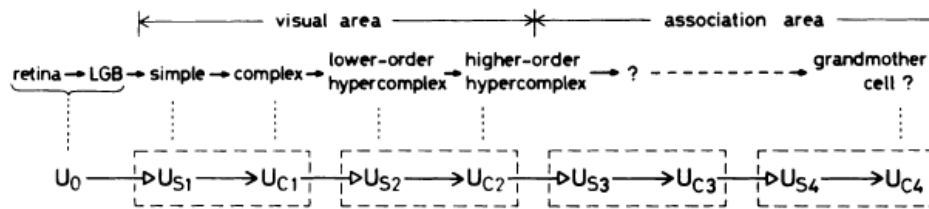


Fig. 1. Comparison between hierarchical model by Hubel and Wiesel and structure of neural network of neocognitron.

828

IEEE TRANSACTIONS ON SYSTEMS, MAN, AND CYBERNETICS, VOL. SMC-13, NO. 5, SEPTEMBER/OCTOBER 1983

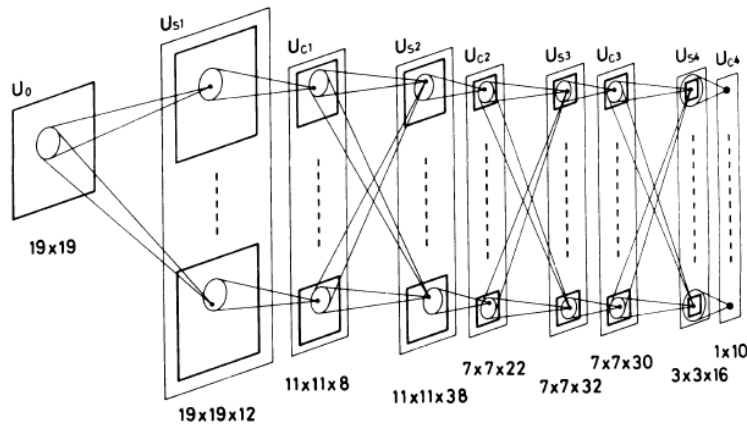


Fig. 2. Schematic diagram illustrating synaptic connections between layers in neocognitron.

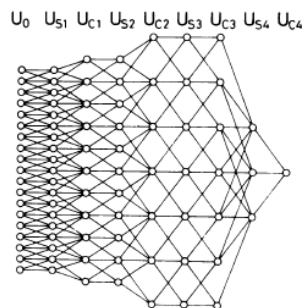


Fig. 3. One-dimensional view of interconnections between cells of different cell planes. Only one cell plane is drawn in each layer.

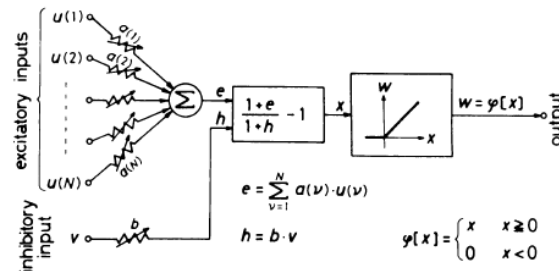


Fig. 4. Input-to-output characteristics of S cell: typical example of cells employed in neocognitron.



Kunihiro Fukushima

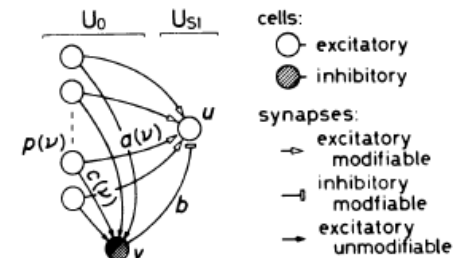


Fig. 5. Synaptic connections converging to S cell.

Yinelemeli Ağ- Recurrent Neural network 1990

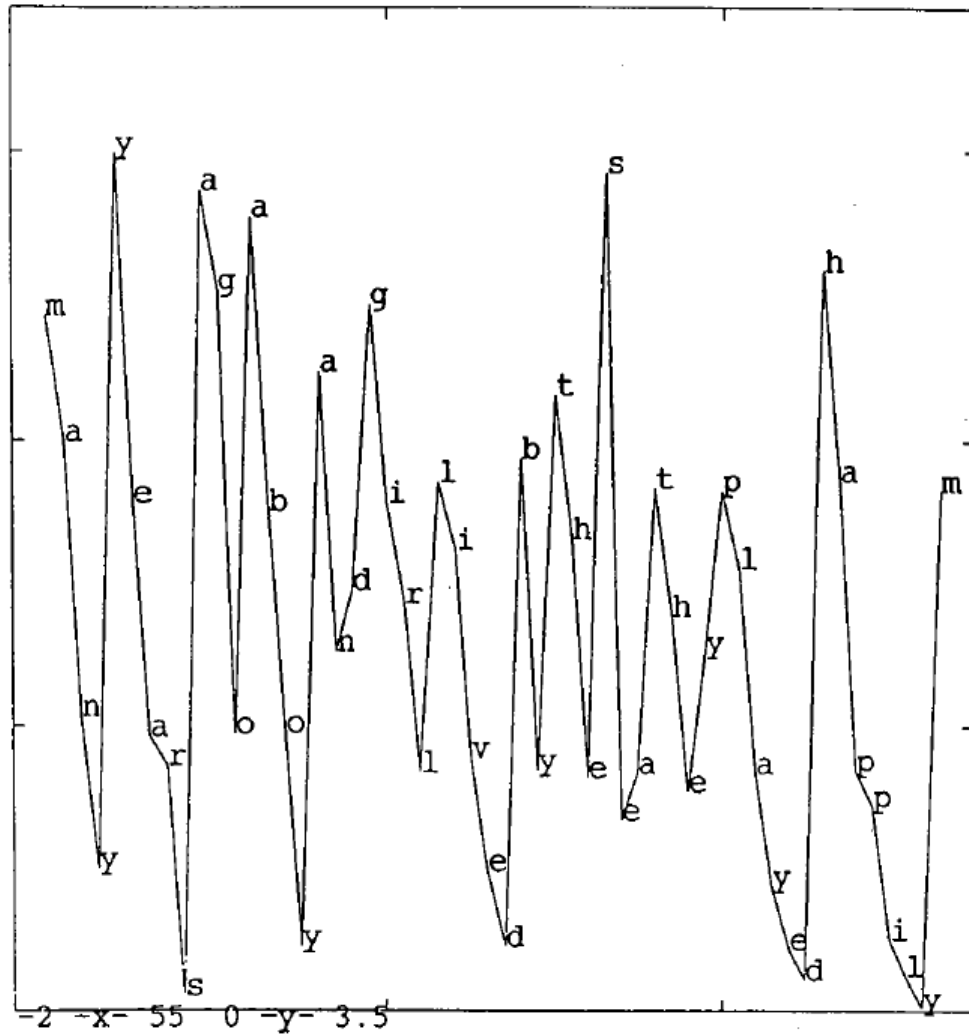
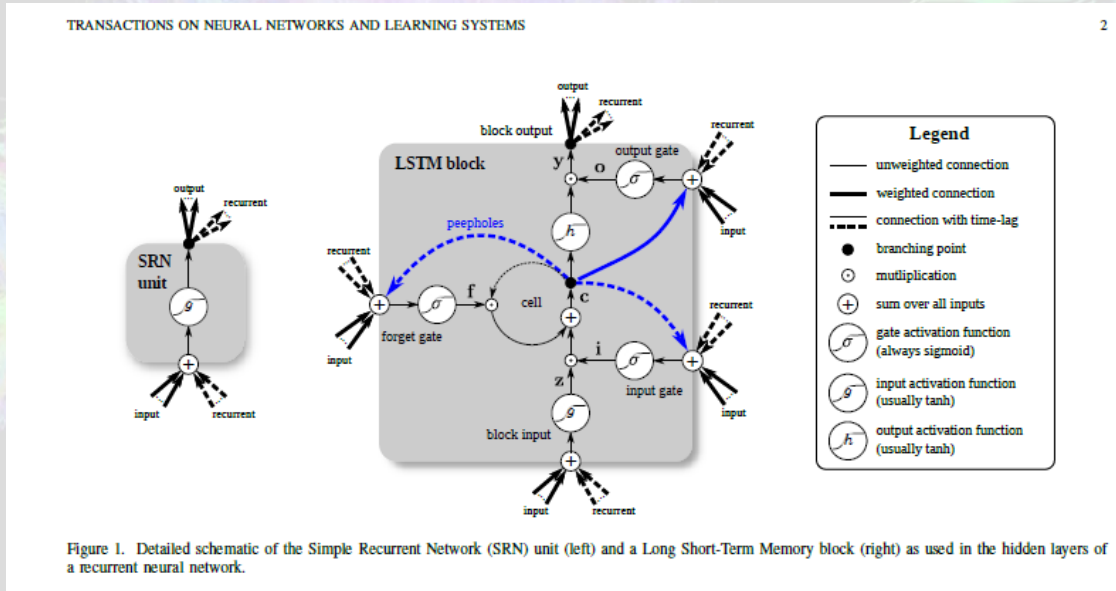


Figure 6. Graph of root mean squared error in letter-in-word precision task.



Jeffrey L. Elman
1948-2018

Long-Short Term Memory 1997



Greff, Klaus, et al. "LSTM: A search space odyssey." *IEEE neural networks and learning systems* (2017)

Jürgen Schmidhuber
1963

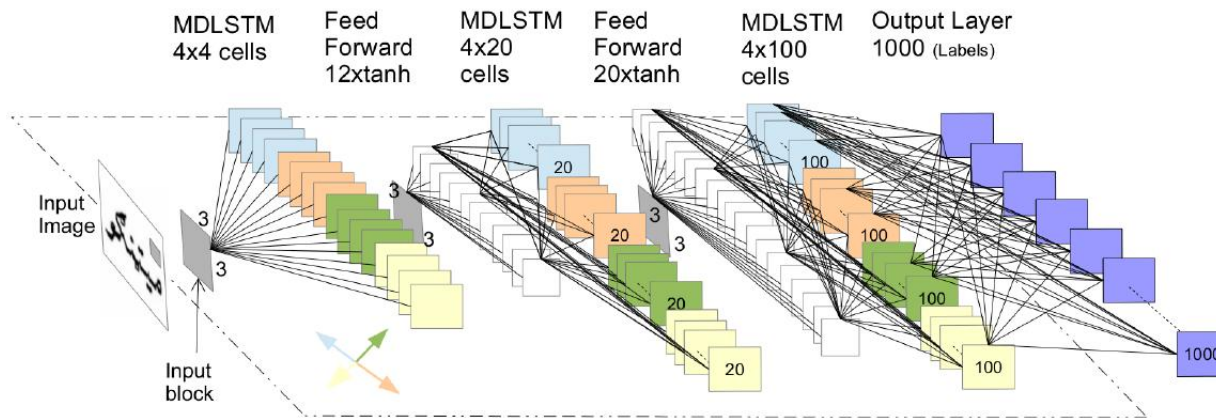


Fig. 5. The proposed 2D-LSTM architecture, with 4, 20 and 100 hidden layers. The 4 different colors in hidden layers; represent the direction in which pixel value has been read. Each cell is fully connected with all cells in the next layer.

Ahmad, Riaz, et al. "Scale and rotation invariant OCR for Pashto cursive script using MDLSTM network." 2015

Katlamalı Ağ Yapıları – Convolutional Neural Networks

ImageNet Classification with Deep Convolutional Neural Networks 2012

Alex Krizhevsky
University of Toronto
kriz@cs.utoronto.ca

Ilya Sutskever
University of Toronto
ilya@cs.utoronto.ca

Geoffrey E. Hinton
University of Toronto
hinton@cs.utoronto.ca

Abstract

We trained a large, deep convolutional neural network to classify the 1.2 million high-resolution images in the ImageNet LSVRC-2010 contest into the 1000 different classes. On the test data, we achieved top-1 and top-5 error rates of 37.5% and 17.0% which is considerably better than the previous state-of-the-art. The neural network, which has 60 million parameters and 650,000 neurons, consists of five convolutional layers, some of which are followed by max-pooling layers, and three fully-connected layers with a final 1000-way softmax. To make training faster, we used non-saturating neurons and a very efficient GPU implementation of the convolution operation. To reduce overfitting in the fully-connected layers we employed a recently-developed regularization method called “dropout” that proved to be very effective. We also entered a variant of this model in the ILSVRC-2012 competition and achieved a winning top-5 test error rate of 15.3%, compared to 26.2% achieved by the second-best entry.



Geoffrey E. Hinton
1947

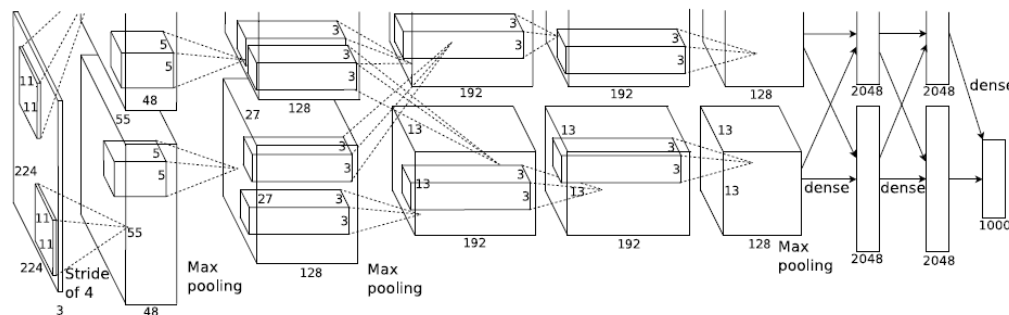


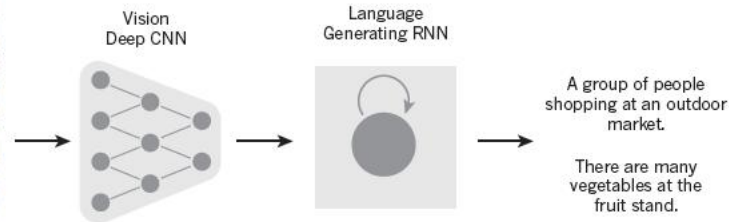
Figure 2: An illustration of the architecture of our CNN, explicitly showing the delineation of responsibilities between the two GPUs. One GPU runs the layer-parts at the top of the figure while the other runs the layer-parts at the bottom. The GPUs communicate only at certain layers. The network's input is 150,528-dimensional, and the number of neurons in the network's remaining layers is given by 253,440–186,624–64,896–64,896–43,264–4,096–4,096–1000.

Deep learning

Yann LeCun^{1,2}, Yoshua Bengio³ & Geoffrey Hinton^{1,2}

Deep learning allows computers to learn from data with multiple levels of abstraction. In visual object recognition, deep learning discovers intricate structures in data and should change its internal parameters as it learns from the previous layer. Deep convolutional neural networks are used for audio, whereas recurrent neural networks are used for text.

INSIGHT REVIEW



A woman is throwing a frisbee in a park.



A dog is standing on a hardwood floor.



A stop sign is on a road with a mountain in the background.



A little girl sitting on a bed with a teddy bear.



A group of people sitting on a boat in the water.



A giraffe standing in a forest with trees in the background.

Figure 3 | From image to text. Captions generated by a recurrent neural network (RNN) taking, as extra input, the representation extracted by a deep convolutional neural network (CNN) from a test image, with the RNN trained to 'translate' high-level representations of images into captions (top). Reproduced

with permission from ref. 102. When the RNN is given the ability to focus its attention on a different location in the input image (middle and bottom; the lighter patches were given more attention) as it generates each word (bold), we found¹⁰² that it exploits this to achieve better 'translation' of images into captions.

Mastering the game of Go with deep neural networks and tree search

David Silver^{1*}, Aja Huang^{1*}, Chris J. Maddison¹, Arthur Guez¹, Laurent Sifre¹, George van den Driessche¹, Julian Schrittwieser¹, Ioannis Antonoglou¹, Veda Panneershelvam¹, Marc Lanctot¹, Sander Dieleman¹, Dominik Grewe¹, John Nham², Nal Kalchbrenner¹, Ilya Sutskever², Timothy Lillicrap¹, Madeleine Leach¹, Koray Kavukcuoglu¹, Thore Graepel¹ & Demis Hassabis¹

The game of Go has long been viewed as the most challenging of classic games for artificial intelligence owing to its enormous search space and the difficulty of evaluating board positions and moves. Here we introduce a new approach to computer Go that uses 'value networks' to evaluate board positions and 'policy networks' to select moves. These deep neural networks are trained by a novel combination of supervised learning from human expert games, and reinforcement learning from games of self-play. Without any lookahead search, the neural networks play Go at the level of state-of-the-art Monte Carlo tree search programs that simulate thousands of random games of self-play. We also introduce a new search algorithm that combines Monte Carlo simulation with value and policy networks. Using this search algorithm, our program AlphaGo achieved a 99.8% winning rate against other Go programs, and defeated the human European Go champion by 5 games to 0. This is the first time that a computer program has defeated a human professional player in the full-sized game of Go, a feat previously thought to be at least a decade away.



South Korean professional Go player Lee Sedol reviews the match after finishing the final match of the Google DeepMind Challenge Match against Google's artificial intelligence program, AlphaGo, in Seoul, South Korea, Tuesday, March 15, 2016. Google's Go-playing computer program again defeated its human opponent in a final match on Tuesday that sealed its 4:1 victory. (Lee Jin-man/AP)

1997'de Garry Kasparov Deep Blue'ya karşı kaybettiğinde IBM'in açıklaması: Deep Blue, yapay zeka kullanıyor mu? Kısaca yanıt 'hayır'dır. İnsan düşünüşünü taklit etmeye çalışan eski bilgisayar tasarımları, bu işte pek iyi değildi. Sezgilere karşılık gelen bir formül yok... Deep Blue daha çok hesaplama gücüne, ayrıca basit arama ve değerlendirme işlevlerine dayanır. Deep Blue uğraşsa bile asla bir HAL-9000 olamaz. Hatta Deep Blue, 'uğraşmak' ne demek onu da bilmez. *

Dopamine neurons report an error in the temporal prediction of reward during learning

Jeffrey R. Hollerman^{1,2} and Wolfram Schultz¹

¹ Institute of Physiology, University of Fribourg, CH-1700 Fribourg, Switzerland

² Present address: Department of Psychology, Allegheny College, Meadville, Pennsylvania, 16335, USA

Correspondence should be addressed to W.S. (Wolfram.Schultz@unifr.ch)

Many behaviors are affected by rewards, undergoing long-term changes when rewards are different than predicted but remaining unchanged when rewards occur exactly as predicted. The discrepancy between reward occurrence and reward prediction is termed an 'error in reward prediction'. Dopamine neurons in the substantia nigra and the ventral tegmental area are believed to be involved in reward-dependent behaviors. Consistent with this role, they are activated by rewards, and because they are activated more strongly by unpredicted than by predicted rewards they may play a role in learning. The present study investigated whether monkey dopamine neurons code an error in reward prediction during the course of learning. Dopamine neuron responses reflected the changes in reward prediction during individual learning episodes; dopamine neurons were activated by rewards during early trials, when errors were frequent and rewards unpredictable, but activation was progressively reduced as performance was consolidated and rewards became more predictable. These neurons were also activated when rewards occurred at unpredicted times and were depressed when rewards were omitted at the predicted times. Thus, dopamine neurons code errors in the prediction of both the occurrence and the time of rewards. In this respect, their responses resemble the teaching signals that have been employed in particularly efficient computational learning models.

Pekiştirmeli Öğrenme – Bir Hesaplamalı Model

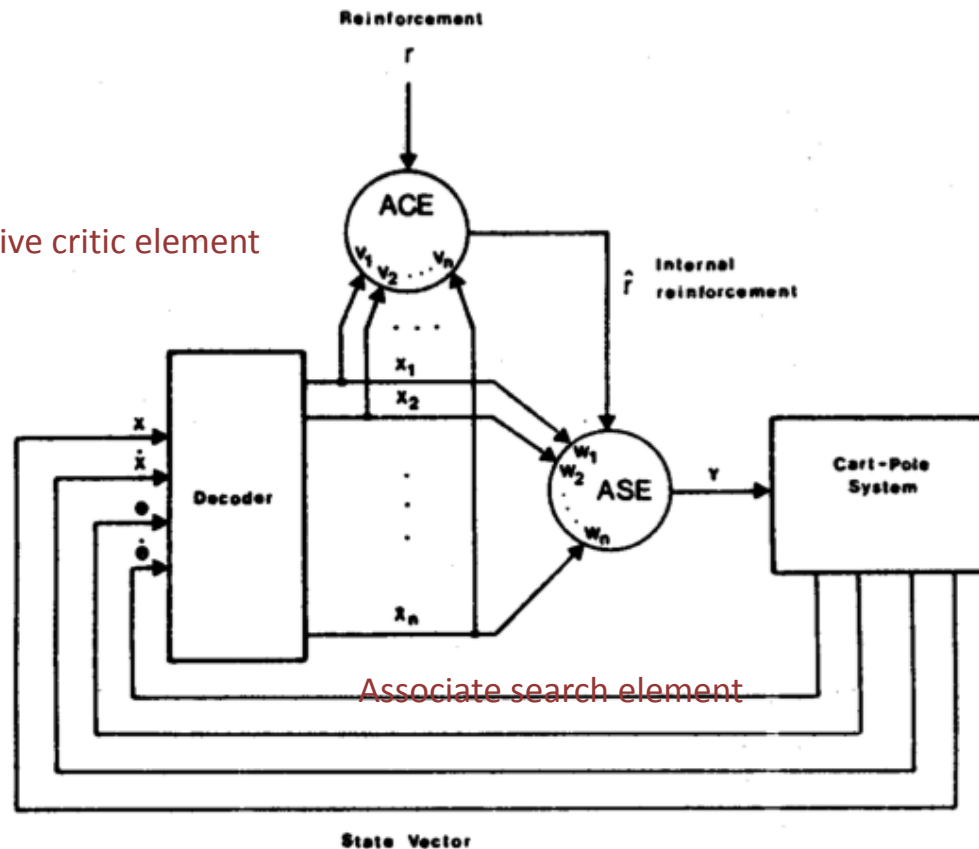
Neuronlike Adaptive Elements That Can Solve Difficult Learning Control Problems

ANDREW G. BARTO, MEMBER, IEEE, RICHARD S. SUTTON, the pole under the conditions usually assumed by control

Abstract—It is adaptive elements to balance a pole on a cart's base. It is as system are not know a failure signal that vertical, or the cart

Manuscript received was supported by Laboratory under C The authors are Science, University

Adaptive critic element

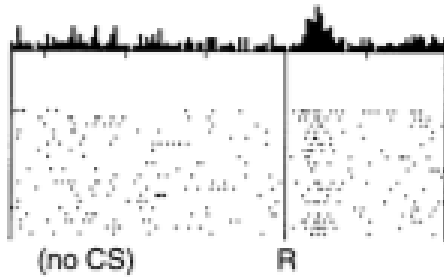


Associate search element

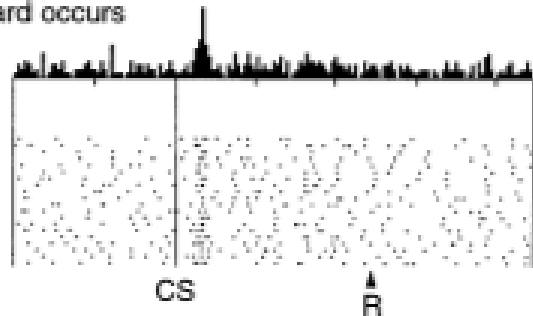
Fig. 3. ASE and ACE configured for pole-balancing task. ACE receives same nonreinforcing input as ASE and uses it to compute an improved or internal reinforcement signal to be used by ASE.

Dopamin nöronları ödülü öngörüyor – bir hesaplamalı model

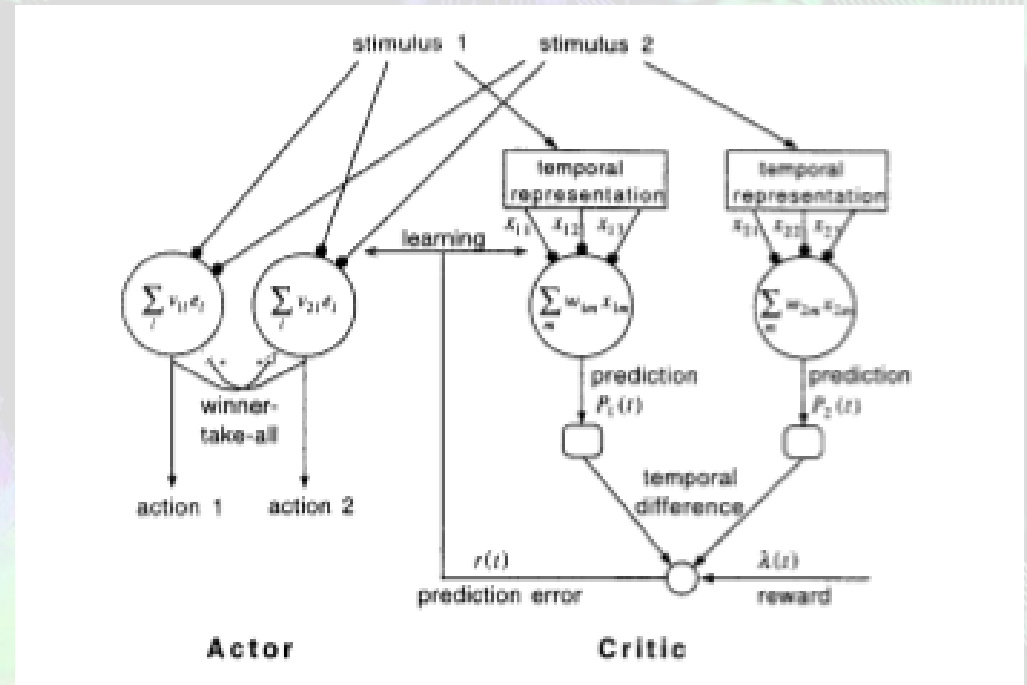
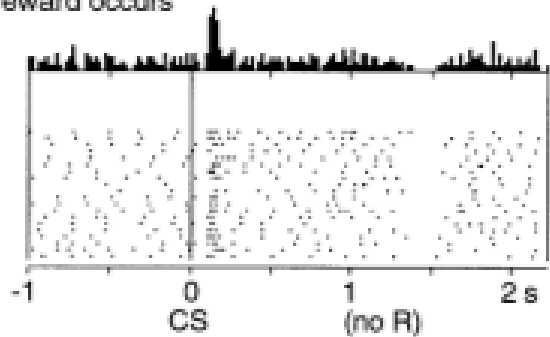
No prediction
Reward occurs



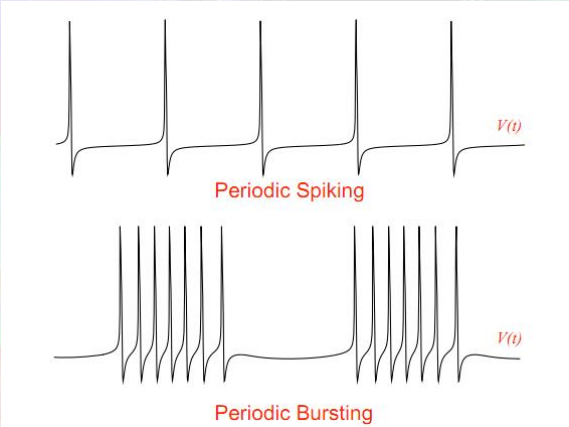
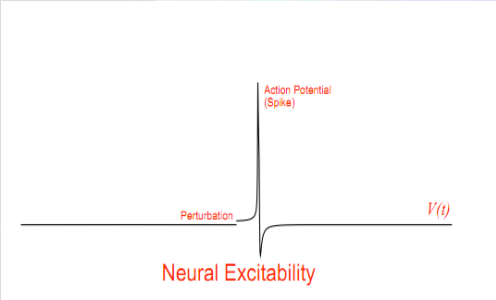
Reward predicted
Reward occurs



Reward predicted
No reward occurs



Hücre davranışlarını açıklayacağımız bir matematik araç var mı?

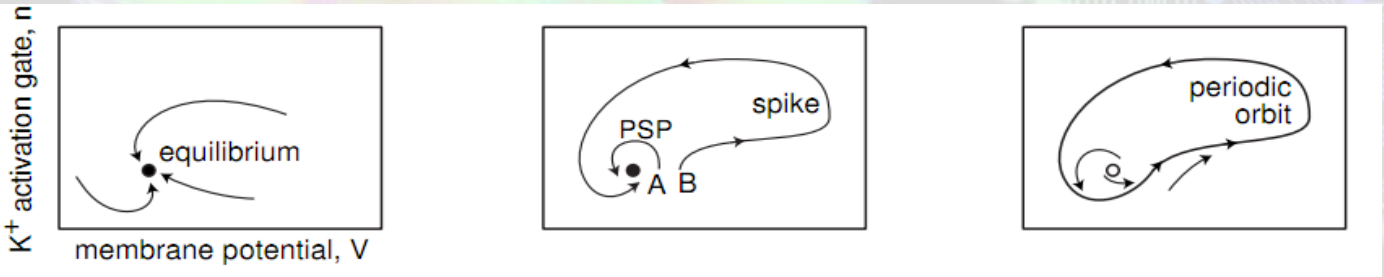
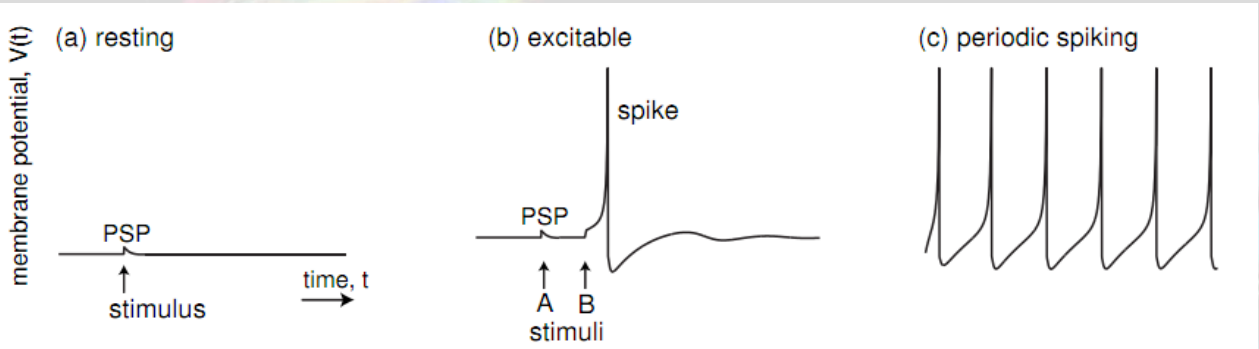


Dallanma (Bifurcation)

$$\frac{dx}{dt} = f(x), \quad x \in \mathbb{R}^n$$

$$\frac{dx}{dt} = f(x, \alpha), \quad x \in \mathbb{R}^n, \quad \alpha \in \mathbb{R}^m$$

Dallanma: Bir parametrenin değişimi ile topolojik olarak eşdeğer olmayan durum portresinin oluşumuna “dallanma” denir.



Matematik sinirbilimde işe yarıyor mu, nasıl?

The J

Activity Patterns in a Model for the Subthalamic the Basal Ganglia

D. Terman,¹ J. E. Rubin,² A. C. Yew,¹ and C. J. Wilson³

Department of Mathematics, The Ohio State University, Columbus, Ohio 43210, University of Pittsburgh, Pittsburgh, Pennsylvania 15260, and ³Division of Life Sciences, San Antonio, Texas 78249

2966 J. Neurosci., April 1, 2002, 22(7):2963-2976

Terman et al. • Subthalamic Activity Patterns

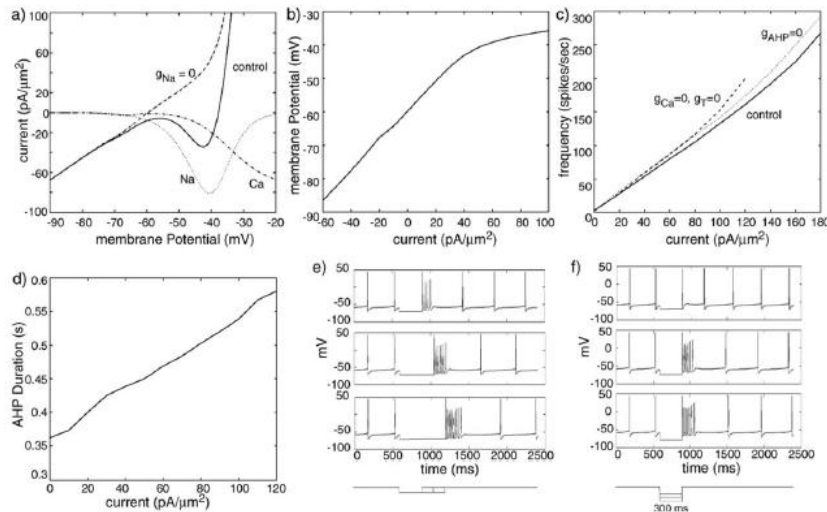


Figure 1. Properties of STN model neuron. *a*, Current as a function of voltage. For fixed voltages, steady-state currents were computed with slow gating variables set to their limiting values ($X \rightarrow X_{\infty}(v)$; see Materials and Methods). In this and all subsequent figures, omitted units are as in Tables 1 and 2. *b*, Membrane potential of a model STN cell under various current injections. The parameter g_{Na} has been set to 0 to mimic the behavior of an STN cell in the presence of sufficient concentration of TTX to block spiking. *c*, Spike frequency as a function of injected current (solid line, full model; dotted line, $g_{AHP} = 0$; dashed line, $g_{Ca} = g_{T} = 0$). *d*, Duration of afterhyperpolarization after high-frequency spiking. A constant current pulse was applied to a model STN cell for 500 msec. After this, a prolonged afterhyperpolarization occurred before the cell returned to regular spiking. Its duration is plotted against the strength of applied current. *e*, *f*, STN rebound bursts after hyperpolarizing injections. *g*, *h*, Model responses of STN cell to currents of varying duration: 25 pA/μm² of current applied for 300 (top), 450 (middle), and 600 (bottom) msec. Longer current application augments deactivation of I_T , enhancing rebound. *i*, Responses to currents of varying magnitude: 20 (top), 30 (middle), and 40 (bottom) pA/μm² of current applied for 300 msec. Stronger current application augments deactivation of I_T , enhancing rebound.

Terman et al. • Subthalamic Activity Patterns

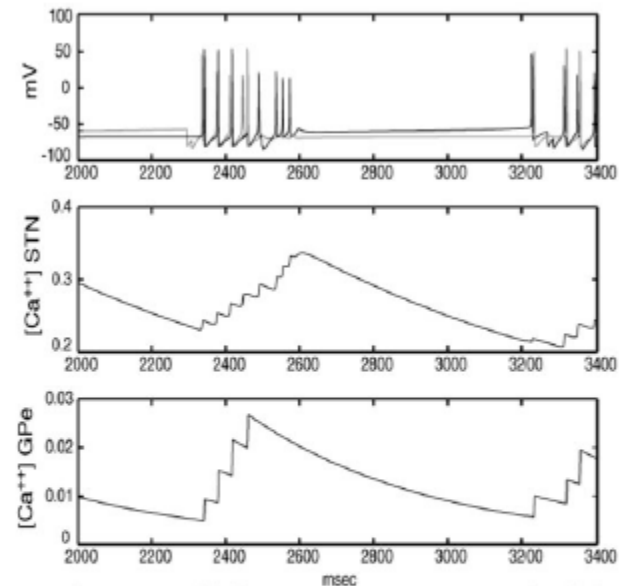


Figure 4. Mechanisms underlying episodic activity patterns. The gray trace in the top box shows the evolution of voltage over time for a single GPe cell in an episodic pattern, whereas the black trace shows the voltage for a single STN cell. The boxes below show the intracellular calcium concentration of each cell as a function of time. Initially, GPe spikes closely follow STN spikes. Here I_{app} is sufficiently strong such that the build-up of calcium terminates the GPe activity of the cell eventually, after which the STN cell fires one last volley of rebound spikes until about 2600 msec. Subsequent decay of calcium allows STN activity to resume after time 3200 msec; this recruits the GPe cell again.

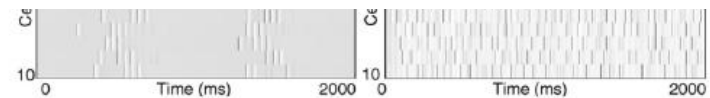


Figure 3. Activity patterns in a random, sparsely connected architecture. *a*, Arrangement of the model network. Each STN neuron excites a single GPe neuron selected at random, and each GPe neuron inhibits three randomly chosen STN cells. GPe cells also inhibit each other through all-to-all connections. *b*, Dependence of activity patterns on coupling strengths $g_{G \rightarrow G}$ and $g_{S \rightarrow G}$. Weak STN \rightarrow GPe excitation or strong GPe \rightarrow GPe inhibition leads to sparse irregular firing patterns. Intermediate values yield episodic patterns, whereas high levels of excitation and low levels of GPe mutual inhibition give rise to continuous uncorrelated activity. *c*, Membrane potential (in millivolts) as a function of time (in milliseconds) for individual cells in each of the activity patterns: sparse activity ($g_{G \rightarrow G} = 0.06$ nS/μm²; $g_{S \rightarrow G} = 0.03$ nS/μm²; $g_{G \rightarrow S} = 2.5$ nS/μm²; $I_{app} = -1.2$ pA/μm²), episodic, almost-synchronized spiking ($g_{G \rightarrow G} = 0$ nS/μm²; $g_{S \rightarrow G} = 0.016$ nS/μm²; $g_{G \rightarrow S} = 2.5$ nS/μm²; $I_{app} = -1.2$ pA/μm²), and continuous, irregular spiking ($g_{G \rightarrow G} = 0.02$ nS/μm²; $g_{S \rightarrow G} = 0.1$ nS/μm²; $g_{G \rightarrow S} = 2.5$ nS/μm²; $I_{app} = -1.2$ pA/μm²). *d*, Network activity in various patterns. In each plot, 10 rows show the voltage traces of 10 cells, with time evolving over 2000 msec to the right along each row. Voltage is coded in gray scale as shown. Because they are so brief, individual action potentials (dark gray line segments) are not prominent, but are more clearly indicated by their afterhyperpolarization (white bars).

Striatal origin of the pathologic beta oscillations in Parkinson's disease

M. M. McCarthy^{a,1}, C. Moore-Kochlacs^{a,2}, X. Gu^{b,2}, E. S. Boyden^c, X. Han^b, and N. Kopell^{a,1}

^aDepartment of Mathematics and Statistics, Boston University, Boston, MA 02215; ^bDepartment of Biomedical Engineering, Photonics Center, Boston University, Boston, MA 02215; and ^cMedia Lab, Massachusetts Institute of Technology, Cambridge, MA 02139

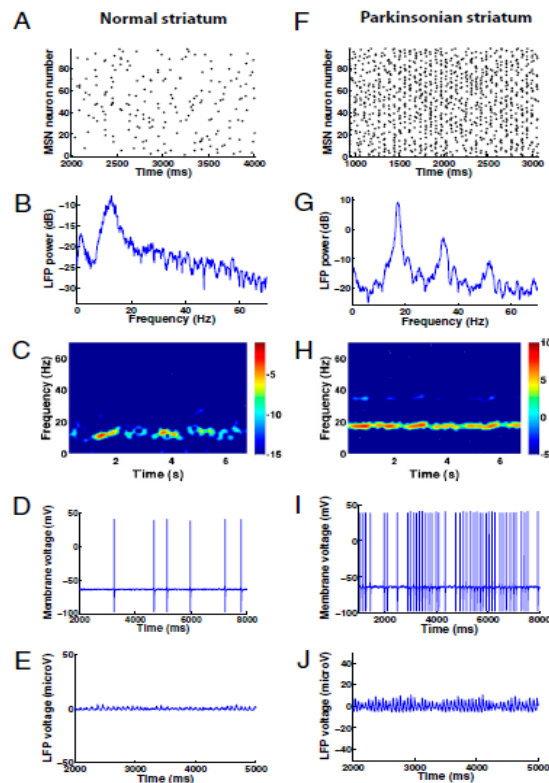


Fig. 1. Beta oscillations emerge in the model striatum under normal conditions and become enhanced under parkinsonian conditions. *A–E* are taken from the same 7-s simulation under normal conditions, and *F–J* are from the same 7-s simulation under parkinsonian conditions. (*A*) Raster plot of 100 reciprocally connected medium spiking neurons (MSNs) under normal, non-parkinsonian conditions. (*B*) Power spectral density of the model LFP. (*C*) Spectrogram of the model LFP. (*D*) Membrane voltage fluctuations from one MSN in the network. (*E*) Waxing and waning of the model LFP trace under normal conditions. (*F*) Raster plot of 100 reciprocally connected MSNs under parkinsonian conditions. (*G*) Power spectral density of the model LFP. (*H*) Spectrogram of the model LFP. (*I*) Membrane voltage fluctuations from one MSN in the parkinsonian network. (*J*) The model LFP trace under parkinsonian conditions.

The results presented here highlight the powerful combination of mathematical and experimental approaches in addressing problems in systems neuroscience. Dynamics of biological systems do not readily yield to direct observation using even the most sophisticated experimental approaches. We show here that informed biophysical modeling can be highly predictive of complex biological dynamics. Additionally, these findings also have broad implications in understanding beta oscillations in normal motor function as well as their inappropriate expression in other disorders with striatal involvement.

Mühendisler ne yapıyor?



BRAINS IN SILICON
STANFORD UNIVERSITY

Home
About our Work
Neurogrid
The Challenge
The Board
The Chip
Projects
People
Lab Positions
Contact
Courses
Publications
Downloads
In the News



On This Page

The Board: Neurogrid

Inspired by **GRAPE-6**, a \$60K supercomputer revolutionized astrophysics, Neurogrid provides an affordable option for brain simulations. It uses computation to **emulate** ion-channel activity **software** synaptic connections. These techniques because they operate in parallel and in serial, constrain the number of distinct ion-channel—unlike digital computation, which simply takes Digital communication constrains the number activated per second—unlike analog communication inputs onto the same wire. Working within the its goal of simulating multiple cortical areas in choices.

Recent breakthroughs in neuromorphic engineering make it possible to combine analog's parallel operation with digital's programmability, reaping the best of both worlds.

Neurogrid simulates one million neurons with two subcellular compartments each, a choice motivated by neurophysiological studies. Nonlinear interactions between projections that terminate in distinct cortical layers have been replicated in a pyramidal-cell model with just **two compartments**. Furthermore, varying the compartments' electrical coupling replicates the firing patterns of various pyramidal-cell types. Capturing these behaviors using the smallest number of compartments minimizes the number of distinct ion-channel populations that need to be simulated, thereby maximizing the number of neurons a model can have.



Neurogrid
With a
(Neu
circuit
model
neuro
interc
spike
Neuro
daugh
and h
respe

Neurogrid simulates a million neurons connected by billions of synapses in real-time, rivaling a supercomputer while consuming a 100,000 times less energy—five watts instead of a megawatt!

frontiers in
NEUROSCIENCE

Neuromorphic silicon neuron circuits

Giacomo Indiveri^{1*}, Bernabé Linares-Barranco², Tara Julia Hamilton³, André van Schaik⁴, Ralph Etienne-Cummings⁵, Tobi Delbruck¹, Shih-Chii Liu¹, Piotr Dudek⁶, Philipp Häflicher⁷, Sylvie Renaud⁸, Johannes Schemmel⁹, Gert Cauwenberghs¹⁰, John Arthur¹¹, Kai Hynna¹¹, Fopeolu Folowosele⁵, Sylvain Saighi⁸, Teresa Serrano-Gotarredona², Jayawan Wijekoon⁶, Yingxue Wang¹² and Kwabena Boahen¹¹

¹ Institute of Neuroinformatics, University of Zurich and ETH Zurich, Zurich, Switzerland

² National Microelectronics Center, Instituto Microelectronica Sevilla, Sevilla, Spain

³ School of Electrical Engineering and Telecommunications, University of New South Wales, Sydney, NSW, Australia

⁴ School of Electrical and Information Engineering, University of Sydney, Sydney, NSW, Australia

⁵ Whiting School of Engineering, Johns Hopkins University, Baltimore, MD, USA

⁶ School of Electrical and Electronic Engineering, University of Manchester, Manchester, UK

⁷ Department of Informatics, University of Oslo, Oslo, Norway

⁸ Laboratoire de l'Intégration du Matériau au Système, Bordeaux University and IMS-CNRS Laboratory, Bordeaux, France

⁹ Kirchhoff Institute for Physics, University of Heidelberg, Heidelberg, Germany

¹⁰ Department of Bioengineering and Institute for Neural Computation, University of California San Diego, La Jolla, CA, USA

¹¹ Stanford Bioengineering, Stanford University, Stanford, CA, USA

¹² Janelia Farm Research Campus, Howard Hughes Medical Institute, Ashburn, VA, USA

Edited by:

Bert Shi, The Hong Kong University of Science and Technology, Hong Kong

Reviewed by:

Theodore Yu, University of California at San Diego, USA

Chi-Sang Poon, Harvard – MIT Division of Health Sciences and Technology, USA

Tadashi Shibata, University of Tokyo, Japan

*Correspondence:

Giacomo Indiveri, Institute of Neuroinformatics, Swiss Federal Institute of Technology Zurich, University of Zurich, Zurich CH-8057, Switzerland.
e-mail: giacomino@ini.phys.ethz.ch

Hardware implementations of spiking neurons can be extremely useful for a large variety of applications, ranging from high-speed modeling of large-scale neural systems to real-time behaving systems, to bidirectional brain-machine interfaces. The specific circuit solutions used to implement silicon neurons depend on the application requirements. In this paper we describe the most common **building blocks and techniques** used to implement these circuits, and present an overview of a wide range of neuromorphic silicon neurons, which implement different computational models, ranging from biophysically realistic and conductance-based **Hodgkin-Huxley models** to bi-dimensional generalized adaptive integrate and fire models. We compare the different design methodologies used for each silicon neuron design described, and demonstrate their features with experimental results, measured from a wide range of fabricated VLSI chips.

Keywords: analog VLSI, subthreshold, spiking, integrate and fire, conductance based, adaptive exponential, log-domain, circuit

<https://web.stanford.edu/group/brainsinsilicon/neurogrid.html>

A reconfigurable on-line learning spiking neuromorphic processor comprising 256 neurons and 12 synapses

Ning Qiao, Hesham Mostafa, Federico Corradi, Marc Osswald, Fabio Stefan Dora Sumislawska and Giacomo Indiveri *

Institute of Neuroinformatics, University of Zurich and ETH Zurich, Zurich, Switzerland

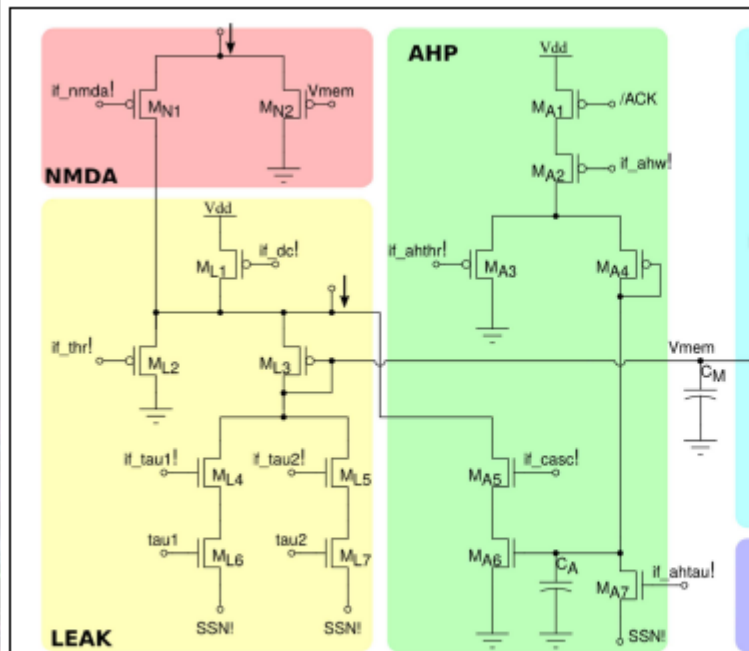


FIGURE 3 | Silicon neuron schematics. The NMDA block implements a voltage gating mechanism; the LEAK block models the neuron's leak conductance; the spike-frequency adaptation block AHP models the effect of the

after-hyper-polarization current. The AHP block models the Pot

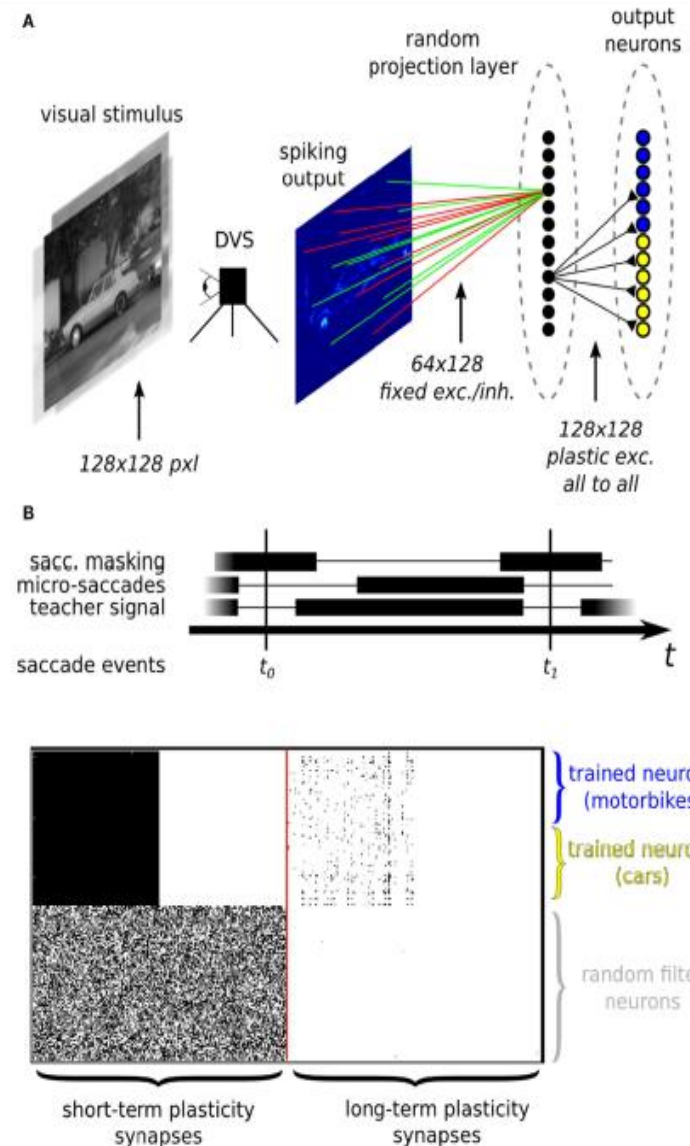


FIGURE 12 | (A) Image classification example using inputs from a DVS. **(A)** Top: neural network architecture. Two different classes of images (here motorbikes or cars) are displayed on a screen with a small jitter applied at 10Hz. A random subset of the spikes emitted by the DVS are mapped to 128 hidden layer neurons. Specifically, each of the 128 neurons is connected to 64 randomly selected pixels with either positive or negative weights, also set at random. The output neurons in the last layer receive spikes from all the 128 hidden layer neurons, via plastic synapses. The output layer neurons are also driven by an external

"teacher" signal which is correlated with one of the image classes. **(A)** Bottom: diagram of the experimental protocol timeline. Notice the presence of a saccade inhibition mechanism which electronically suppresses DVS input during a virtual saccade, i.e., when the displayed image is replaced with the next one. **(B)** Synaptic matrices of the ROLLS neuromorphic processor showing the hardware configuration of the classification neural network. The STP synapses represent the synapses of the hidden layer; the LTP synapses represent the synapses of the output layer.

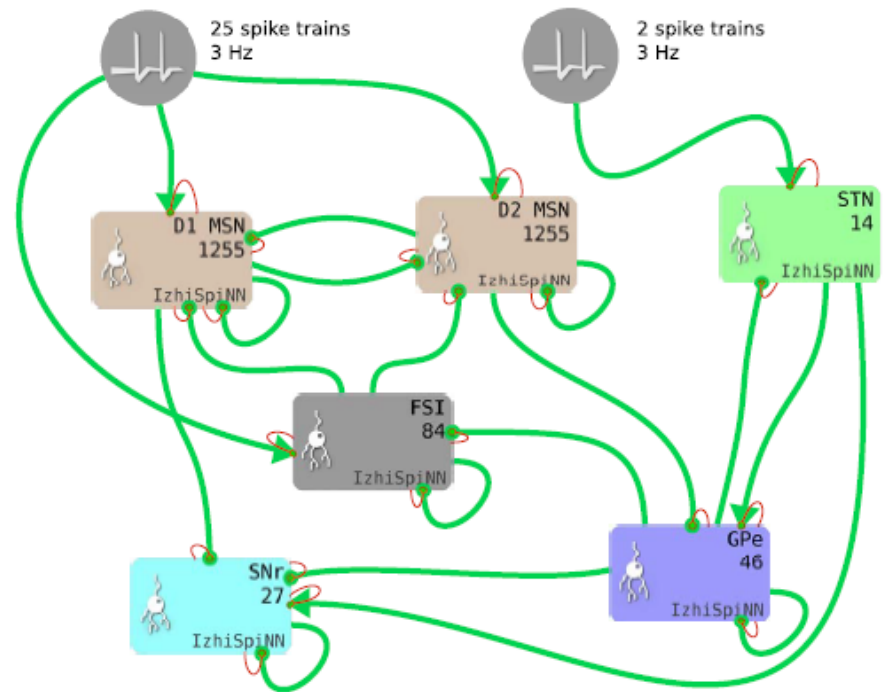
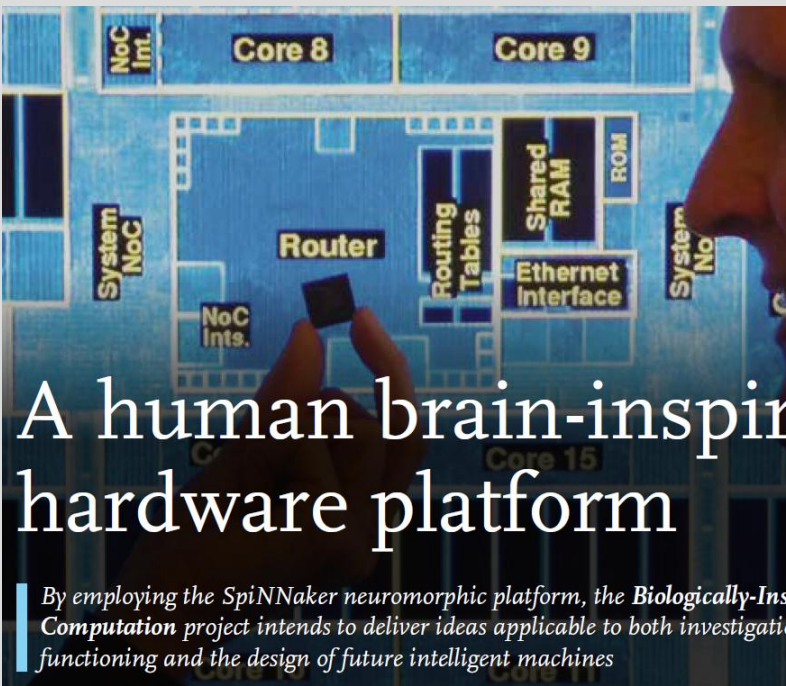
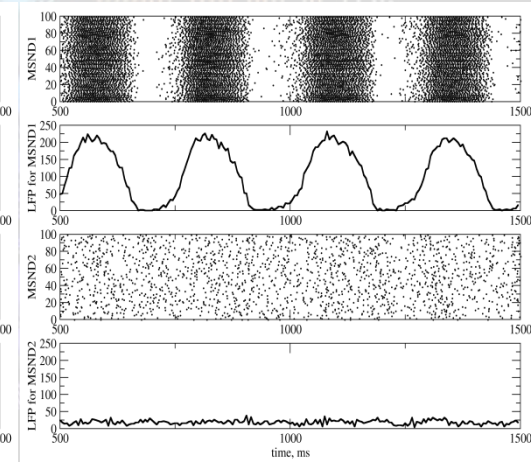
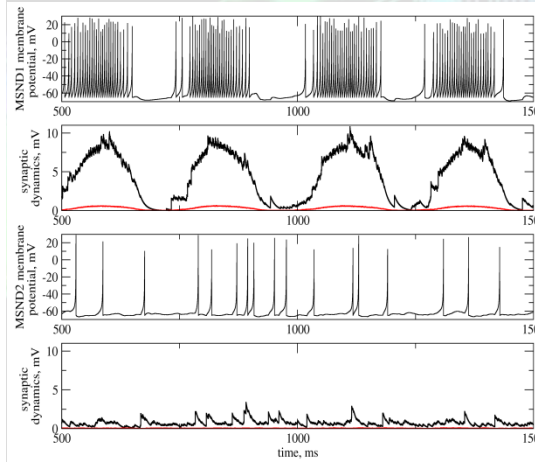
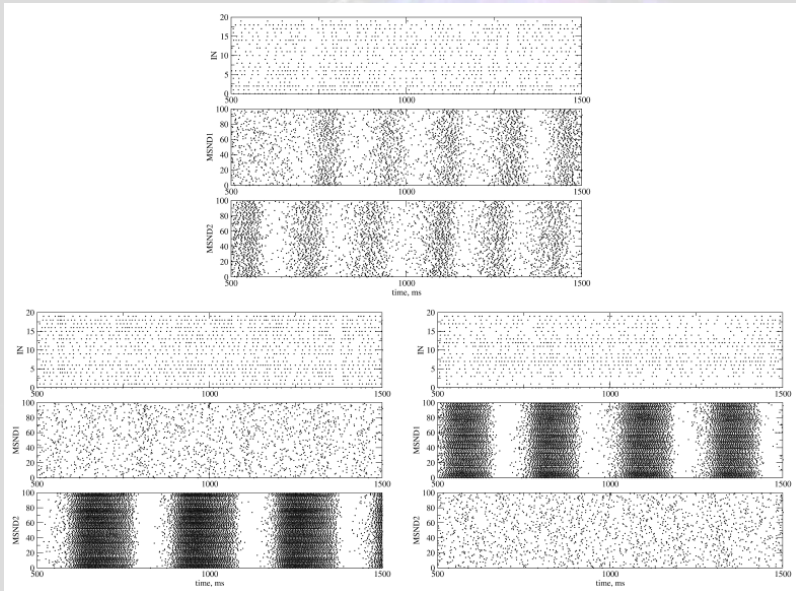
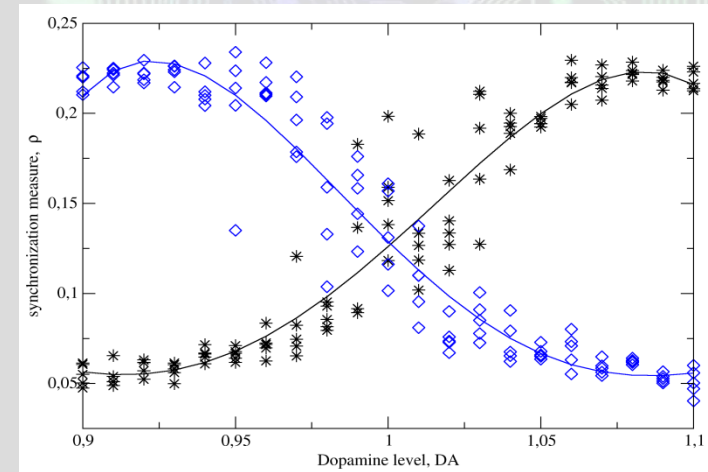
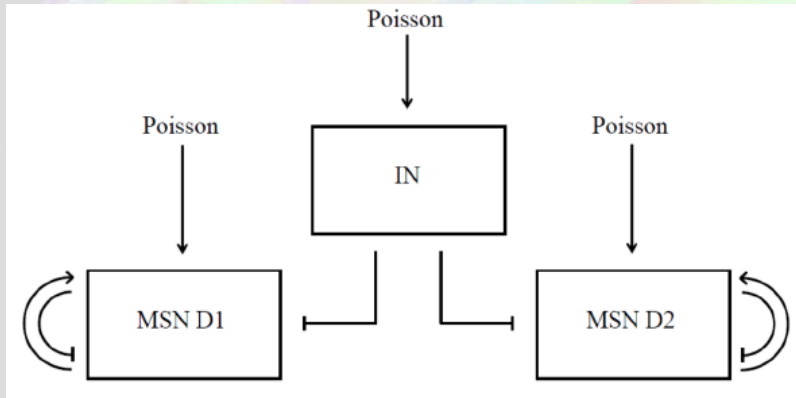
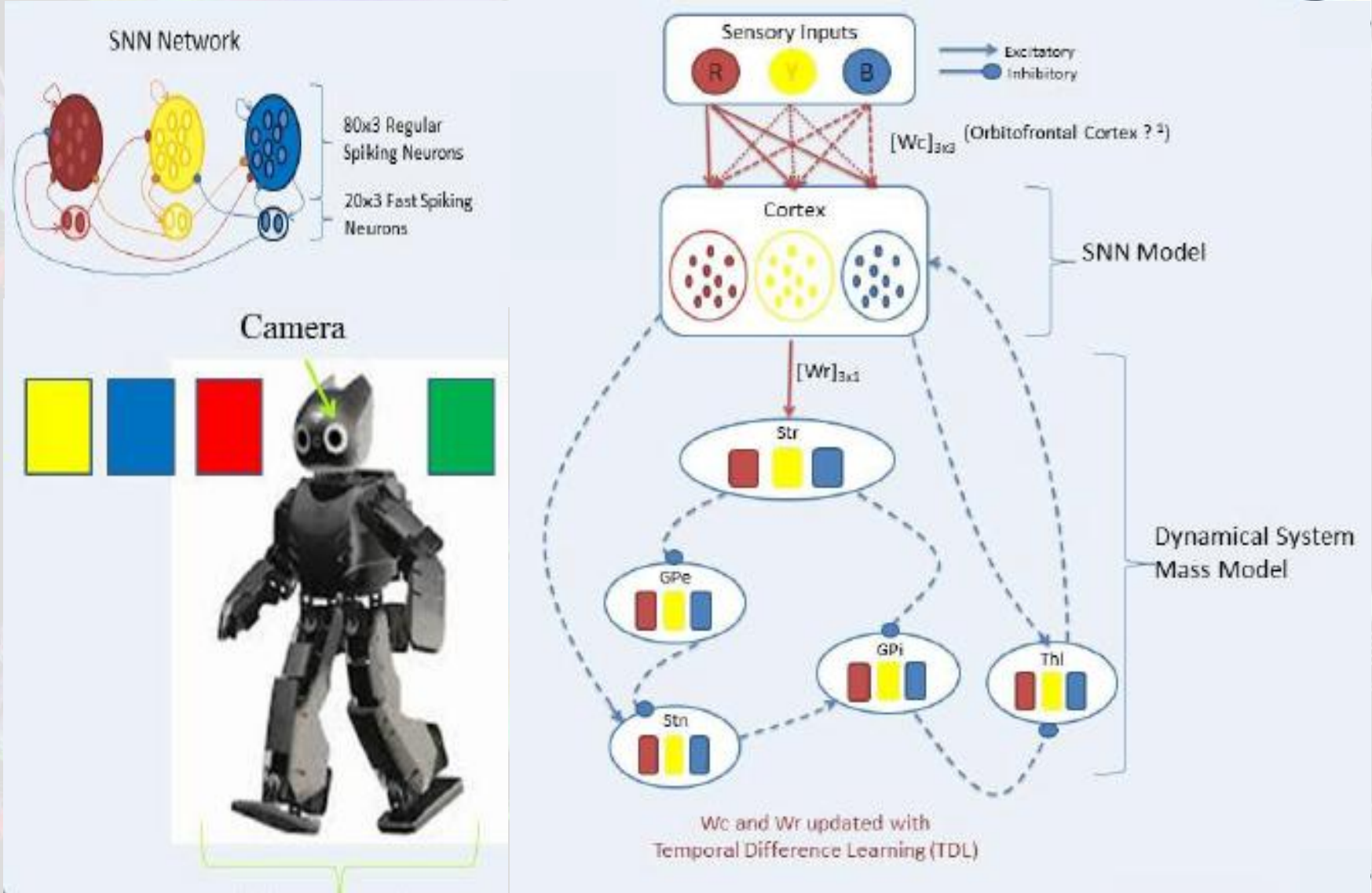


Fig. 3. Single-channel BG network, as exported from SpineCreator. Rectangular boxes are neural populations. The population name, number of elements, and SpineML component are shown in the box. Gray circles represent Poisson spike train sources. Green arrows are projections with element to element connectivities that are parameterized as in the SpiNNaker-based model and reported in Tables I–III. Projections with arrow heads are excitatory, those with circles for heads are inhibitory. The thinner, red lines which connect populations to arrowheads connect the membrane voltage variable $v(t)$ [defined in (1)] in the efferent population to the synapse component in each projection (on a one to one basis), allowing the synaptic current to be computed.

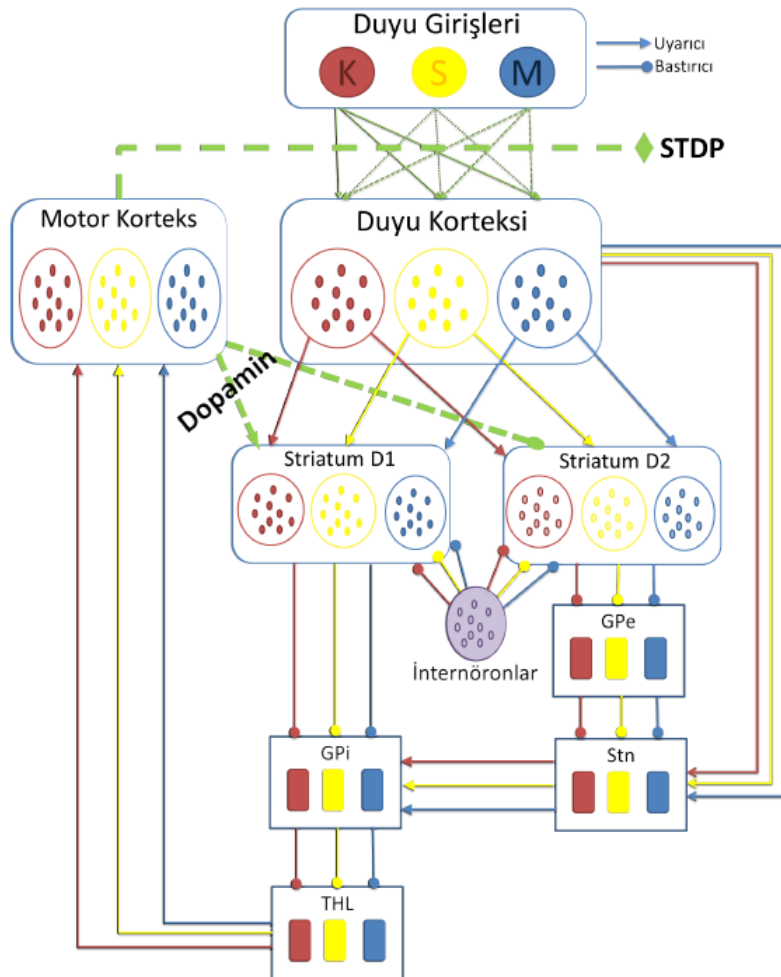
Striatumdaki Senkronizasyona Dopaminin Etkisine Dair Bir Hesaplamalı Model



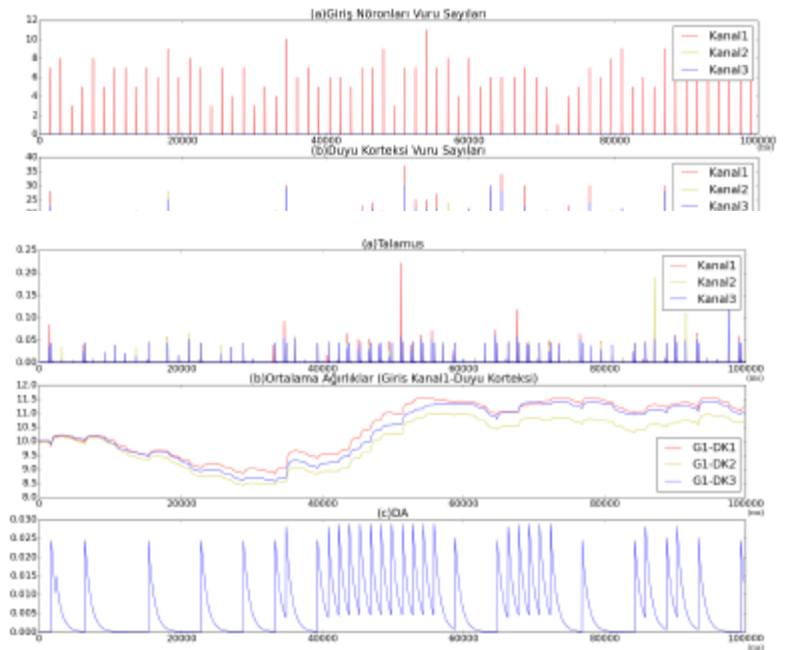
Hareket Seçimini Öğrenme



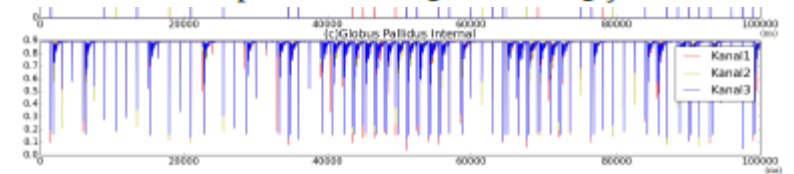
Uyaran Hareket Seçiminin Oluşmasına dair bir Model



Şekil 1: Ödüle dayalı eylem seçimine ilişkin model.

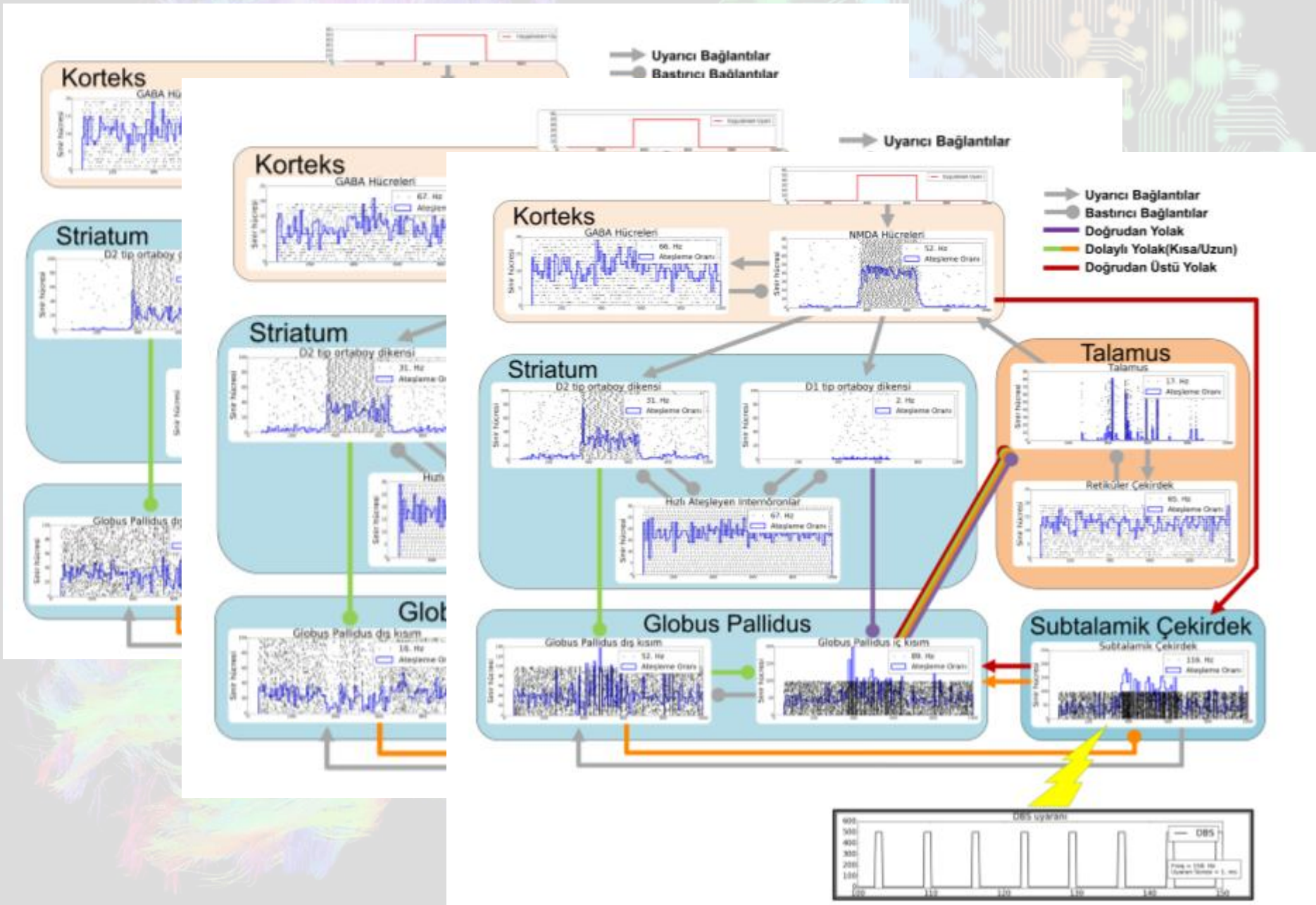


Şekil 4: (a): Talamus yığın modeli değerleri. (b): Duyu girişleri ile duyu korteksi kanalları arasındaki bağlantı ağırlıkları. (c): Verilen ödül ile dopamin (DA) değerindeki değişim.



Şekil 3: (a): Striatum D1, (b): D2 nöronları vuru sayıları. (c): Globus Pallidus İnternal yığın modeli değerleri.

Parkinson ve derin beyin uyarımı





Teşekkürler.....